Manuscript title

Pharmacological assessment of sepiapterin reductase inhibition on tactile response in the rat

Authors and affiliations

James T. Meyer, Brian A. Sparling, William J. McCarty, Maosheng Zhang, Marcus Soto, Stephen Schneider, Hao Chen, Jonathan Roberts, Helming Tan, Thomas Kornecook, Paul Andrews, Charles G. Knutson.

Amgen Research, One Amgen Center Drive, Thousand Oaks, CA 91320, United States (JTM, MZ, MS, HT, TK)

Amgen Research, 360 Binney Street, Cambridge, MA 02142, United States. (BAS, WJM, SS, HC, JR, PA, CGK)

JPET 257105

Running Title:

PK/PD relationship with sepiapterin reductase inhibition

Corresponding Author:

Charles G. Knutson

Amgen Research

Department of Pharmacokinetics and Drug Metabolism

Amgen Inc.

360 Binney Street

AMA1/4-G-10

Cambridge, MA 02142

Tel. 617.444.5470

E-mail: charlie.knutson@amgen.com

Numbers:

Text pages: 34

Number of tables: 3

Number of figures: 4

Number of references: 27

Number of words in Abstract: 241

Number of words in Introduction: 652

Number of words in Discussion: 1262

JPET 257105

Nonstandard abbreviations:

AA, Ascorbic Acid

ALS, autosampler

BH4, Tetrahydrobiopterin

BIO, 6-Biopterin

CAD, collision activated dissociation

CE, collision energy

CI, confidence interval

CUR, curtain gas

CXP, collision cell exit potential

DMSO, Dimethyl Sulfoxide

DP, declustering potential

DRG, dorsal root ganglion

FA, Formic Acid

GCH1, GTP cyclohydrolase 1

HCl, Hydrochloric Acid

HPLC, high performance liquid chromatography

I, Iodine

IS, Internal Standard

3

i.v., intravenous

KI, Potassium Iodide

MSA, methyl sulfonic acid

K_2EDTA, di-potassium ethylenediaminetertra-acetic acid

LC-MS/MS, liquid chromatography tandem mass spectrometry

NH_4OH, Ammonium Hydroxide

RHAM, Rhamnopterin [6-(L-1,2,3-Trihydroxybutyl)-pterin]

RP, reverse phase

SEP, L-Sepiapterin

SNL, spinal nerve ligation

SPR, Sepiapterin Reductase

TOL, Tolbutamide

VER, Verapamil-HCl

Recommended section assignment:

Drug Discovery and Translational Medicine

Abstract

There is an unmet medical need for non-opioid pain therapies in human populations; several pathways are under investigation for possible therapeutic intervention. Tetrahydrobiopterin (BH4) has received attention recently as a mediator of neuropathic pain. Recent reports have implicated sepiapterin reductase (SPR) in this pain pathway as a regulator of BH4 production. To evaluate the role of SPR inhibition on BH4 reduction, we developed analytical methods to monitor the relationship between the plasma concentration of test article and endogenous pterins and applied these in the rat spinal nerve ligation pain model. Sepiapterin is an endogenous substrate, which accumulates upon inhibition of SPR. In response to a potent inhibitor of SPR, plasma concentrations of sepiapterin increased proportionally with exposure. An indirect effect PK/PD model was developed to describe the relationship between the plasma PK of test article and plasma sepiapterin levels in the rat, which was used to determine an in vivo SPR IC_{50} value. Evaluation of SPR inhibition and mechanical allodynia was assessed coordinately with pterin biomarkers in plasma and at the site of neuronal injury (i.e., dorsal root ganglion). Upon QD p.o. administration for 3 consecutive days, unbound plasma concentrations of test article exceeded the unbound in vivo rat SPR IC_{90} throughout the dose intervals leading to a 60% reduction in BH4 in the dorsal root ganglion. Despite evidence for pharmacological modulation of the BH4 pathway, there was no significant effect on the tactile paw withdrawal threshold relative to vehicle-treated controls.

Introduction

Chronic pain affects close to 300 million people in the U.S. annually. Due to the lack of therapeutic options, one common pharmacological intervention is to prescribe opioids. The mortality rate from opioid overdose exceeds 90 Americans per day (Rudd et al., 2016). Over-prescription of opioids (such as fentanyl) leads to misuse and addiction that has an increasing burden on societal and health care systems(Volkow et al., 2014). In effort to reduce the production and use of opioid analgesics, the pharmaceutical industry is investigating alternative biological pathways of pain reduction, which has led to the rapid prosecution and validation of new pain targets. Accordingly, several putative targets for analgesia have emerged in recent years; of particular interest are enzymes that regulate tetrahydrobiopterin (BH4) synthesis. BH4 is reported to enhance pain sensitivity in the dorsal root ganglia (DRG) in preclinical models with associated links to human pain(Latremoliere and Costigan, 2011; Latremoliere et al., 2015). Subsequently, drug discovery and development efforts have emerged to reduce BH4 by developing inhibitors of biosynthetic enzymes involved in BH4 biosynthesis (Tebbe et al., 2017).

BH4 is an essential cofactor for several enzymes (nitric oxide synthase and aromatic amino acid hydrolases) and its production occurs through de novo synthesis and enzymatic salvage pathways in vivo (Latremoliere and Costigan, 2011). GTP cyclohydrolase 1 (GCH1) is elevated during chronic pain and performs the rate-limiting step in de novo synthesis of BH4 by converting GTP to 7,8-dihydroneopterin-triphosphate (Hatakeyama et al., 1991; Tegeder et al., 2006). Sepiapterin reductase (SPR), which is also elevated during chronic pain, is involved in both de novo biosynthesis and scavenging pathways(Tegeder et al., 2006; Latremoliere and Costigan, 2011) (Figure 1). Since GCH1 is a master regulator of BH4 production in vivo, inhibition of GCH1 is likely to significantly reduce systemic BH4 levels, which may lead to undesirable biological consequences. Therefore, the downstream enzyme, SPR, has emerged as a more desirable target to reduce BH4 levels because several SPR-catalyzed steps in BH4 production are also catalyzed by other enzymes (Latremoliere and Costigan, 2011; Latremoliere et al., 2015). Recent efforts have focused on development of SPR inhibitors that would lead to reduction of BH4 but not its complete elimination. As due diligence to assess new targets in the discovery pipeline for neuropathic pain, we recently evaluated candidate

inhibitors of SPR. To evaluate our conviction in the target it was necessary to benchmark internal efforts to those reported in the literature. Therefore, we developed bioanalytical methods to quantify components of the BH4 biosynthesis pathway to guide our interpretation of pharmacodynamic response related to SPR inhibition in preclinical behavior models of tactile allodynia.

Using available literature reports, our objective was to develop low-volume, high-throughput analytical methods for the quantitation of BH4, biopterin (BIO), sepiapterin (SEP), and test article in both plasma and DRG tissues to quickly make decisions regarding the advancement of molecules. Multiple bioanalysis methods have been reported for quantitation of BH4, BIO and SEP (Stea et al., 1980; Schmidt et al., 2006; Fismen et al., 2012; Kim et al., 2012; Arning and Bottiglieri, 2016). The stability of BIO and SEP allow these molecules to be analyzed by routine protein precipitation methods. However, BH4 is susceptible to autoxidation, which complicates its direct analysis. Our bioanalytical approach developed two separate analysis arms to account for: 1, direct measurement analytes (BIO, SEP, test article); 2, indirect measurement of BH4 via oxidative stabilization to BIO. A total of 6 assays were developed to measure biomarkers and test article in both plasma and DRG matrixes (Figure 2). These efforts were designed to support early discovery portfolio with efficient use of resources; thus, the analytical assays were developed as fit-for-purpose without the requirement of analytical method validation (Cummings et al., 2008; Administration, 2013; Leonard et al., 2014; Cowan et al., 2016). These biomarker assays for BH4, BIO and SEP were successfully employed for the quantitative measurement of target engagement (SPR inhibition) in preclinical PK and PK/PD studies.

Methods

Chemicals

Dimethyl Sulfoxide (DMSO), Water for HPLC, Methanol for HPLC, Isopropanol, Acetonitrile for HPLC, Formic Acid (88-91%), Hydrochloric Acid (37%), Iodine (99.8%), Potassium Iodide USO 99%, Ascorbic Acid, Ammonium Hydroxide (28-30%), BH4, 6-Biopterin, SEP, Verapamil-HCl (VER), Tolbutamide (TOL), gabapentin and methyl sulfonic acid were obtained from Sigma-Aldrich (Saint Louis, MO, U.S.). BH4 was obtained from Combi Blocks (San Diego, CA, U.S.). Rhamnopterin (RHAM), was obtained from Carbosynth Ltd (Berkshire, UK). Tween 80 was obtained from Croda (East Yorkshire, UK). Hydroxy propyl methyl cellulose (HPMC), 50 cps grade, was obtained from Spectrum Chemicals (New Brunswick, NJ, U.S.). Sprague-Dawley rat K_2EDTA plasma and DRG were obtained from BioreclamationIVT (Westbury, NY, U.S.).

Chemical Synthesis of SPRi3 and Q-1195

SPRi3 was synthesized in 2 steps from 5-methoxy-2-methyltryptamine via stepwise *O*-demethylation and *N*-acylation with 2-methoxyacetic acid. The synthesis is further described in the Supplemental Methods.

Q-1195 was identified from U.S. Patent 2017/0096435 and a synthetic route was designed (Tebbe et al., 2017). Briefly, selective hydrolysis of 2,4-dichloropyrrolotriazine followed by nucleophilic displacement with hydrazine afforded the intermediate hydrazinylpyrrolotriazinone. The condensation product of methyl acetoacetate with dimethylformamide dimethyl acetal was then coupled with the hydrazinylpyrrolotriazinone to afford the methyl pyrazolecarboxylate intermediate, which was saponified to the corresponding carboxylic acid in preparation for amide formation. The amine coupling partner was prepared via reductive amination of Boc-protected diazabicyclo[3.1.1]heptane with 1,1,-ethoxy(trimetylsilyl)cyclopropane, followed by Boc deprotection. Amide formation of the acid with the amine afforded Q-1195. The synthesis is further described in the Supplemental Methods.

Instrumentation and LC-MS Conditions

BIO and SEP LC-MS/MS. The HPLC system contained the following modules: CBM20A controller; solvent degassing unit; 2 LC20ADXR pumps; SIL30ACMP temperature-controlled autosampler; CTO30A column oven (Shimadzu, Kyoto, Japan). Chromatographic separation was achieved on a Phenomenex Synergi 4μ Polar RP (80A, 50 x 2 mm) column maintained at 40°C. Mobile phase A consisted of water with 0.002% FA and mobile phase B consisted of methanol with 0.002% FA. The gradient profile was as follows: 0.0 to 0.2 min at 0% B; 0.2 to 1.2 min linear increase to 10% B; 1.2 to 1.3 min linear increase to 100% B; 1.3 to 1.95 min hold at 100% B; 1.95 to 2.0 min return to 0% B; 2.0 to 2.5 min hold at 0% B. The total run time was 2.5 min at a flow rate of 0.5 ml/min. Samples were kept at 15°C in the autosampler. Twenty μl of sample extract was injected with the column effluent plumbed to an AB Sciex 4000 triple quadrupole mass spectrometer (AB Sciex, Framingham, MA, U.S.). The mass spectrometer was operated in negative ion mode turbo spray with the following parameters: CUR at 20, GS1 and GS2 at 30, gas temperature at 500°C, CAD gas at 12, ion spray voltage at -4500 V and entrance potential at -10 V. Tuning parameter settings were optimized by post-column infusion of 1 μg/ml analyte at 1 to 5 μl/ml into a flow of 0.1 ml/min 50% B. All biomarker analytes and internal standards were scanned in multiple reaction monitoring (MRM) mode using the parameter settings shown in Supplemental Table 1. Analyst version 1.6.1 software (AB Sciex, Framingham, MA, U.S.) was used for HPLC control, data acquisition and initial data processing.

Q-1195 LC-MS/MS conditions. Chromatographic separation was achieved on a Phenomenex Synergi 4μ Polar RP (80A, 50 x 2 mm) column maintained at 40°C. Mobile phase A consisted of water with 0.002% FA and mobile phase B consisted of methanol with 0.002% FA. The gradient profile was as follows: isocratic hold of 5% B from 0.0 to 0.15 min; linear increase to 100% B from 0.15 to 0.75 min; isocratic hold at 100% B from 0.75 to 1.25 min; linear decrease to 5% B from 1.25 to 1.3 min; isocratic hold (re-equilibration) at 5% B from 1.3 to 1.7 min. The total run time was 1.7 min at a flow rate of 0.6 ml/min. Samples were kept at 15°C in the autosampler over the course of analysis. Two μl of sample extract was injected with the column effluent in line with an AB Sciex 4000 triple quadrupole mass spectrometer. The mass spectrometer was operated in positive ion mode turbo spray with the following parameters: CUR at 20, GS1 and GS2 at 30, gas temperature at 500°C, CAD gas at 12, ion spray voltage at 4500 V and entrance potential at 10 V. Tuning parameter settings

were optimized by post-column infusion of 1 µg/ml analyte at 1 to 5 µl/ml into a flow of 0.1 ml/min 50% B.

Analyte and internal standard were scanned in MRM mode using the parameter settings shown in

Supplemental Table 2.

Compound Stock Solutions

BH4, BIO, SEP, RHAM, Q-1195, VER and TOL were weighed in duplicate and dissolved in DMSO:methanol

(1:1) at 1.0 mg/ml as free base. RHAM required addition of 20 mM HCl to solubilize. Prior to use, the duplicate

1.0 mg/ml stock solutions were analyzed with multiple injections (n = 6); the mean area was determined for

each stock solution and, if within 20%, then aliquoted at 50 µl per tube and stored at -70°C for up to 4 months.

Standard and Sample Preparation and Analysis

Homogenization of DRG. Due to the challenges in handling the small DRG tissues (1 to 2 mg per DRG), DRG

L4, L5 and L6 from the ipsilateral side were pooled; separately, DRG L4, L5 and L6 from the contralateral side

were pooled from each subject on study. The pooled DRGs were weighed and 9-times their weight in water

was added, representing a 10-fold dilution of the matrix and providing sufficient volume for subsequent sample

preparation steps. Homogenization of the DRGs was accomplished using two 3 mm tungsten carbide beads

per sample in snap cap tubes and processing in the TissueLyzer (Qiagen, Hilden, Germany) with a frequency

of 15 cycles/s for 5 min.

Selection of stock solution solvent. There are varied literature reports of solvents used to prepare stock

solutions of BH4, BIO and SEP. Stock solutions (1.0 mg/ml) were prepared by weighing in duplicate in the

following solvents: water, 25 mM HCl in water, DMSO and DMSO:Methanol (1:1) (Fukushima and Nixon,

1980a; Zhao et al., 2009; Fismen et al., 2012). DMSO:Methanol (1:1) showed a near 10-fold increase in MS

signal. Subsequently, all stock solutions were prepared in DMSO:Methanol (1:1). Stock solution aliquots (50

µL) in individual tubes were capped and stored at -70°C. Stock solution stability was established out to 4

months under these conditions.

Rat plasma. Endogenous levels of BIO and SEP were evaluated in 6 individual lots of blank K_2EDTA rat

plasma using this method. BIO levels were BQL (< 2.5 ng/ml) in 4 of 6 lots; the remaining 2 lots contained 11

and 55 ng/ml of BIO. The lots with less than 2.5 ng/ml were reserved for use as blank matrix. SEP levels were

BQL (< 1 ng/ml) in all 6 individual lots of K_2EDTA rat plasma. These results are similar to previous literature

reports (Fukushima and Nixon, 1980a; Schmidt et al., 2006; Latremoliere et al., 2015).

Preparation of standard curves. To facilitate high-throughput analysis of Q-1195, BIO and SEP, both standards

and samples were prepared in 96-well deep block microtiter plates (Microliter Analytical, Suwanee, GA).

Standard curve concentrations at 1.0, 2.5, 5, 10, 25, 50, 100 and 250 ng/ml were prepared in control Sprague-

Dawley rat K_2EDTA plasma. The Tecan D300e was used to dispense analyte from 100 µg/ml stock solution in

DMSO:Methanol (1:1) into wells containing 20 µl of control plasma. Standard curve concentrations at 10, 15,

25, 50, 100, 250, 500 and 1000 ng/g in DRG homogenate (1:10 diluted in water prior to homogenization) were

prepared using the Tecan D300e to dispense analyte from 100 µg/ml stock solution in DMSO:Methanol (1:1)

into 20 µl of control DRG homogenate.

Bioanalysis of test article, BIO and SEP. For determination of Q-1195, BIO and SEP in both plasma and DRG

matrixes, standards and samples were processed as follows: to 20 µl sample, 150 µl of IS was added (VER

and TOL at 25 ng/ml in ACN), vortexed for 30 s and then centrifuged for 5 min at 3200 x g in a Beckman-

Coulter Allegra 25R centrifuge (Danvers, MA, U.S.). A Tomtec Quadra 4 liquid handling system was used to

transfer 125 µl of supernatant to a fresh 96-well deep block microtiter plate. The supernatant was taken to

dryness under 15 psi N_2 gas at 60°C. The dry down procedure required 50 min in an UltraVap (Porvair

Sciences, Wrexham, UK). Standards and samples were reconstituted in 100 µl of mobile phase A, sealed with

a pre-slit 96-round-well sealing mat (Phenomenex, Torrance, CA), vortexed for 1 min on a plate shaker (VWR

VX-2500, Manasquan, NJ) and placed in the autosampler.

Bioanalysis of BH4. Autoxidation of BH4 to BIO can complicate direct assessment of BH4 in biological

matrixes. Stabilization of BH4 in its reduced form immediately upon sample collection has been

reported(Fukushima and Nixon, 1980a; Zhao et al., 2009), but due to limited sample volumes and sizes,

sample processing in this manner was determined to be impractical for routine analysis. Other well-established

reports oxidize BH4 all the way to BIO and indirectly determine BH4 levels by quantitation of BIO (Schmidt et

al., 2006); this method was adopted in our analysis. Correspondingly, a separate analysis arm that

implemented solid-phase extraction (SPE) was incorporated into our procedure to remove these oxidizing reagents from downstream workflow so as not to interfere with the stability of other analytes. Plasma and DRG standards and samples were processed as follows: 20 µl sample was combined with 100 µl of RHAM (25 ng/ml in 0.1 M HCl) then vortexed for 30 s. Fifty µl of oxidizing reagent (10 mg/ml I in 20 mg/ml KI in water) was added to this mixture, vortexed for 30 s and incubated for 30 min at room temperature in the dark. To stop the reaction, 100 µl of ascorbic acid at 50 mg/ml in water was added and the plate(s) were vortexed for 30 s. Note that on addition of ascorbic acid the standards and samples went colorless. Both the ascorbic acid and iodine solutions were made fresh immediately before use.

SPE method for BH4 bioanalysis. Oasis MCX 96-well 30 µm/30 mg plates (Waters, Wexford, Ireland) were prepared as follows: 1.0 ml of methanol was added and washed through each well with positive pressure (~ 1.0 psi). This was followed by 1.0 ml of water that was washed through each well being careful to ensure that a small amount of water remained to cover the column head. The oxidized BH4 standards and samples were transferred to the plate and loaded under ~ 1.0 psi positive pressure. The plates were washed with 1.0 ml of 0.1 M HCl followed by 1.0 ml of methanol. BIO, from oxidized BH4, was eluted with two 250 µl additions of 8% NH_4OH in 25% methanol in water. The eluates were collected into a fresh 96-well plate and taken to dryness under N_2 gas (15 psi) at 60°C for 1 h. Standards and samples were reconstituted in 100 µl of mobile phase A, sealed with a pre-slit 96-round-well sealing mat (Phenomenex, Torrance, CA), vortexed for 1 min on a plate shaker (VWR VX-2500, Manasquan, NJ,) and placed in the autosampler. Standard curve concentrations at 10, 15, 25, 50, 100, 250, 500 and 1000 ng/ml in Sprague-Dawley rat K_2EDTA plasma were prepared using the Tecan D300e dispenser and dispensed BH4 from 100 ug/ml stock solution in DMSO:Methanol (1:1) into wells containing 20 µl of blank plasma. Standard curve concentrations at 10, 15, 25, 50, 100, 250, 500 and 1000 ng/g in DRG homogenate (1:10 diluted in water prior to homogenization) were prepared using the Tecan D300e dispenser and dispensed BH4 from 100 µg/ml stock solution in DMSO:Methanol (1:1) into 20 µl of control homogenate. Standard curves were oxidized and applied to the SPE for wash and elution as described above for the sample analysis.

Standard curve parameters. Standard curves were acquired at the beginning and end of each analytical run. Standard curve linear regression fitting was performed in Watson version 7.4.2 using $1/X^2$ weighting. The inter-assay precision [(S.D./mean)*100] and accuracy [(measured/nominal)*100] of the standard calibrators across multiple analytical runs are reported in Supplemental Table 3. Supplemental Table 4 summarizes the standard curve performance in both plasma and DRG matrices.

Fractional Binding

Pooled plasma and brain homogenates from male Sprague-Dawley rats were obtained from BioIVT (Hicksville, NY). Plasma was treated with lithium heparin and each homogenate was prepared as 1 g of tissue per 4 ml of phosphate-buffered saline. Plasma or homogenate (1 ml) was spiked with test article to a final concentration of 5 µM. Triplicate 200 µl aliquots were transferred to 220 µl ultracentrifuge tubes and spun at 37°C and 190,000 x g for 4.5 h in a Type 42.2 rotor (Beckman Coulter). Twenty-five µl aliquots of spiked matrix were transferred to a sample plate and kept on ice to represent total drug. The remainder of spiked plasma was incubated at 37°C for the duration of the centrifugation period and used as a stability control. After centrifugation, 25 µl aliquots of the unbound fractions were transferred to the sample plate. Twenty-five µl aliquots of the stability control plasma were also transferred to the sample plate. All samples were matched with an equal volume of blank matrix. Samples were extracted by adding 3 volumes of acetonitrile containing internal standard (1 µM TOL) and 0.1% formic acid. Samples were vortexed, centrifuged at 4°C for 15 min at 3400 x g and analyzed by LC-MS using a Thermo Q-Exactive in positive ion mode.

Fraction unbound (f_u) was calculated from the ratio of test article detected in the water layer after centrifugation relative to the total concentration in the original matrix. The f_u in tissue homogenates was corrected for dilution according to the equation described by Kalvass(Kalvass et al., 2007):

$$f_{u2} = \left(\frac{(\frac{1}{D})}{\left(\left(\left(\frac{1}{f_{u1}}\right)-1\right)+(\frac{1}{D})\right)} \right)$$

where f_{u2} is the adjusted fraction unbound in tissues, f_{u1} is the estimated fraction unbound assuming no dilution, and D is the fold-dilution of the tissue.

Formulation

Q-1195 was formulated as a solution of 2 mg/ml in dimethyl sulfoxide (DMSO, Sigma-Aldrich, St. Louis, MO) for intravenous (i.v.) bolus administration in rats. A platform p.o. formulation vehicle of 2% (w/v) hydroxypropylmethylcellulose (HPMC, 50 cps grade, Spectrum Chemicals) and 1% (w/v) Tween 80 (Croda, East Yorkshire, UK) in water was used, and Q-1195 was formulated as an in-situ salt in the vehicle by adjusting to pH 2 with methyl sulfonic acid (Sigma-Aldrich, St. Louis, MO) for oral administration in rats.

In Vivo Experiments

Animals were cared for in accordance to the *Guide for the Care and Use of Laboratory Animals, 8th Edition* (National Research Council (U.S.). Committee for the Update of the Guide for the Care and Use of Laboratory Animals. et al., 2011). Animals were individually or group-housed at an Association for Assessment and Accreditation of Laboratory Animal Care, an internationally accredited facility, in static or ventilated caging on corn cob bedding. All research protocols were approved by the Institutional Animal Care and Use Committee. Animals had ad libitum access to pelleted feed (Harlan 2020X, IN, USA) and reverse osmosis-purified water via water bottles or automatic watering system. Animals were maintained on a 12:12 hour light:dark cycle in rooms at 18 to 26°C and a 30 to 70% humidity range and had access to enrichment opportunities. All animals were determined free of specific pathogens (http://www.criver.com/files/pdfs/rms/hmsummary.aspx). Animals were allowed at least 1 week acclimation to the facility prior to any procedures.

Pharmacokinetic In Vivo Experiments

A total of 18 surgically-modified male Sprague-Dawley rats (8 to 12 weeks old) were obtained from Charles River Laboratories (CA, USA). Rats that were to receive i.v. administration had a femoral vein catheter for dosing and a jugular vein catheter for blood sampling. Rats that were to receive p.o. administration via gavage had only a jugular vein catheter for blood sampling. Rats were arbitrarily assigned to treatment groups (n = 3 rats/group) and received either a single 1 mg/kg i.v. bolus dose of Q-1195 administered at a dose volume of 0.5 ml/kg in 100% DMSO or a single 5, 15 or 45 mg/kg p.o. dose of Q-1195 administered at a dose volume of 10 ml/kg in 2% HPMC, 1% Tween 80, pH 2 adjusted with MSA. Q-1195 was also administered orally once

daily at 15 mg/kg over 3 subsequent days to a group of rats. For single-dose studies, blood was collected at 0.083 (i.v. treatment group only), 0.25, 0.5, 1, 2, 4, 6, 8 and 24 h post-dose. For multiple-dose studies, blood was collected on Day 1 and Day 3 at 0.25, 0.5, 1, 2, 3, 4, 6, 8 and 24 h post-dose. Blood specimens were mixed in SARSTEDT Microvette® K_3EDTA plasma separation tubes and centrifuged at 4°C at 14,000 x g for 5 min to generate plasma. In multiple-dose studies, lumbar DRG (L4, L5 and L6) were harvested from 2 sub-groups of rats at 3 h post-dose on Day 1 and Day 3 immediately following carbon dioxide asphyxiation. DRG L4, L5 and L6 from the ipsilateral side were pooled and DRG L4, L5 and L6 from the contralateral side were pooled, weighed, and frozen. All plasma and DRG specimens were maintained at -70°C (± 10°C) prior to quantitative analysis. Non-compartment analysis was applied to the plasma concentration versus time results to determine pharmacokinetic parameters.

PK/PD Modeling of Q-1195 Exposure to SPR Inhibition

Phoenix WinNonlin/NLME (Certara USA, Princeton, NJ) software was used for the PK and PK/PD modeling. Parameter imprecision was estimated using 95% confidence intervals (CI) around the mean estimates. The plasma PK after single administration i.v. (1 mg/kg) and p.o. (5, 15 and 45 mg/kg) dosing was consistent with a linear extravascular one-compartmental model with first-order elimination. Because lower than dose-proportional plasma PK were observed at the 45 mg/kg dose, bioavailabilities were estimated for each dose and the doses were adjusted for bioavailability when fitting the PK/PD model. Sequential PK/PD model fitting was performed for animals with plasma SEP data. A standard indirect effect model (inhibition of dissipation) (Mager et al., 2003) was used to describe the effect of Q-1195 on the time-course of SEP in plasma with I_{max} fixed at 1. This model is consistent with the anticipated mechanism of Q-1195 inhibiting the conversion of SEP to BH4 by SPR, with the plasma levels of SEP as the PD biomarker. The PK/PD model and best-fit parameters to the 5, 15 and 45 mg/kg data sets were used to project the plasma concentrations of Q-1195 and SEP following 60 mg/kg p.o. dose administered during the open-field activity and SNL studies (described below).

Rat Open-field Activity

Male Sprague-Dawley rats were habituated in a reversed light cycle room in home cages for at least 1 week and acclimated to the testing room for 1 h prior to dosing. Animals were counterbalanced to n = 8 per treatment groups. Q-1195 (15 and 60 mg/kg) or vehicle (2% HPMC, 1% Tween 80, pH 2.2, with MSA) was administered 3 h before placing an animal in the open-field apparatus. Open-field activity was measured using a system that counts interruptions of a set of photobeams for the course of 30 min (Kinder Scientific, Poway, CA). To begin a session, animals were removed from the home cage and placed individually into an independent Plexiglas box (41 L x 41 W x 38 cm H) surrounded by a frame consisting of 32 photocells (16Y and 16X) that track the movement of the animal. Photobeam breaks were used as an indication of activity and were measured as the following parameters per min: basic movements (counts) and total rearing (counts). Following completion of behavioral measurements, animals were euthanized with carbon dioxide followed by immediate blood collection via cardiac puncture for pharmacokinetic analysis (approximately 3.5 h post-dose). Blood collections were mixed in SARSTEDT Microvette® K_3EDTA plasma separation tubes and centrifuged at 4°C at 14,000 x g for 5 min to generate plasma. All plasma and DRG specimens were maintained at -70°C (± 10°C) prior to LC-MS/MS analysis. All behavioral data was scored by an automated device.

SNL-induced Tactile Allodynia

Adult male Sprague-Dawley rats weighing 120 to 150 g were obtained from Harlan (CA, USA) and kept in the reversed light cycle for the entire study. SNL surgeries were performed under a stereomicroscope using standard aseptic surgical techniques as described previously (Kim and Chung, 1992). Spinal nerve injury was caused by ligating the left L5 and L6 (ipsilateral) spinal nerves with special care taken to avoid damage to the L4 spinal nerve. Briefly, under gaseous anesthesia with a mixture of O_2 and isoflurane (4% for induction and 2% for maintenance), skin was excised and longissimus lumborum muscle and the fascia above L6 spinal nerves were carefully removed. These procedures provided a clean and spacious working area to enable complete resection of the L6 transverse process and to separate the L5 from L4 spinal nerve. The L5 and L6 spinal nerves were each tightly ligated with 6-0 silk suture. The entire surgical procedure beginning with skin incision and ending with wound clipping of the skin lasted 7 min or less.

SNL Behavioral Testing

Two weeks post-operation, mechanical sensitivity was measured by determining the median 50% ipsilateral hind paw withdrawal threshold for von Frey filaments using the up-down method. Rats were placed under a plastic cover (9 x 9 x 20 cm) on a metal mesh floor (Chaplan et al., 1994). von Frey filaments (Semmes-Weinstein monofilaments, Stoelting, Wood Dale, IL) were applied to the middle glabrous area between the footpads of the plantar surface of the injured hind paw. This plantar area was touched with a series of nine calibrated von Frey filaments with approximately exponentially incremental bending forces (von Frey filament numbers: 3.61, 3.8, 4.0, 4.2, 4.41, 4.6, 4.8, 5.0 and 5.2; equivalent to 0.41, 0.63, 1.0, 1.58, 2.51, 4.07, 6.31, 10 and 15.8 g). The von Frey filament was presented perpendicular to the plantar surface with sufficient force to cause slight bending and held for approximately 3 to 4 s. To avoid possible reflex responses, only abrupt withdrawal of the foot accompanied by pain-indicative behaviors (namely paw flinching, shaking or licking for more than 2 s) was recorded as a response. Any post-surgery rat that displayed a mechanical threshold of more than 3.16 g or less than 0.7 g was eliminated from the study.

After measuring basal threshold, animals were randomized into 4 groups (a minimum of 10 animals per group) and treated orally with either vehicle (single-dosed), Q-1195 (60 mg/kg, single-dosed or multi-dosed once per day for 3 days) or gabapentin (100 mg/kg, single-dosed). Measurement of the tactile threshold was assessed at 3 h post-dose for Q-1195-treated and vehicle groups, and at 1 and 2 h post-dose for gabapentin-dosed animals. Following completion of behavioral measurements, animals were euthanized with carbon dioxide followed by immediate blood collection via cardiac puncture for pharmacokinetic analysis (approximately 3.5 h post-dose). Lumbar DRGs (L4, L5 and L6) from the ipsilateral side of individual animals were collected and pooled in 1.5 ml microcentrifuge tubes; separately, DRG L4, L5 and L6 from the contralateral side were pooled from each subject into microcentrifuge tubes. Blood collections were mixed in SARSTEDT Microvette® K_3EDTA plasma separation tubes and centrifuged at 4°C at 14,000 x g for 5 min to generate plasma. All plasma and DRG specimens were maintained at -70°C (± 10°C) prior to LC-MS/MS analysis.

Human and Rat SPR Protein Production

SPR cloning and expression. Human (NM_003124.5) and rat (NM_019181.1) sepiapterin reductase genes were synthesized by Integrated DNA Technologies (IDT) and cloned into pET28 vector (Millipore Sigma)

containing an N-terminal FLAG tag followed by thrombin cleavage site. The sequence confirmed expression

constructs were transformed into BL21(DE3) and subsequently a single colony of each construct was

inoculated into 60 ml Terrific Broth (TB) medium supplemented with 50 µg/ml kanamycin. The overnight

cultures were used to inoculate 6 l of TB/kanamycin at a 1:100 v/v ratio. The cultures were grown at 37°C by

shaking at 250 rpm until OD_{600} of ~ 1.0; protein expression was then induced by the addition of 0.5 mM IPTG

(isopropyl-β-D-1-thiogalactopyranoside) for 3 h. Cells were pelleted by centrifugation, washed once with TBS

(20 mM Tris pH 8, 150 mM NaCl) and frozen at -80°C until protein purification.

SPR protein purification. Frozen cells were resuspended in TBS with protease inhibitor cocktail (Roche) and

lysed by a microfluidizer. Cell debris was removed by centrifugation at 40,000 rpm at 4°C using a Beckman

Coulter Ti75 rotor. The cleared cell lysates were incubated with 3 ml of anti-FLAG M2 resin (Sigma-Aldrich)

overnight at 4°C with gentle nutation. Resin was packed into a gravity column and washed with 20 column

volumes of TBS, and proteins were then eluted with 20 ml TBS supplemented with 0.15 mg/ml 3X FLAG®

peptide (Sigma-Aldrich). SPR proteins were further purified by size-exclusion chromatography using a HiLoad

16/60 Superdex-200 column equilibrated in Buffer B (20 mM MES pH 6.5, 100 mM NaCl). SPR-containing

fractions were pooled and concentrated to ~ 0.5 mg/ml using Amicon Ultra-15 filters with 10 kDa MWCO.

Biochemical Assessment of SPR Binding

A low volume high throughput NADP/NADPH-Glo™ Assay (Promega, Madison, WI) was developed to

measure the NADPH dependent SPR reduction of SEP to 7,8-dihydrobiopterin. The conversion of NADPH to

NADP is proportional to the conversion of SEP to 7,8 dihydrobiopterin by SPR. NADP/NADPH-Glo™

technology generates a luminescent signal upon reaction with reductase reducing the proluciferin substrate to

luciferin. Luciferin is then detected with Ultra-Glo™ rLuciferase (Promega, Madison, WI) where the light

generated is proportional to the NADPH in the sample. Inhibition of SPR is assessed by the inhibition of

luciferin signal in response to increasing concentrations of inhibitor.

Assay plates were prepared by dispensing either human FLAG-SPR or rat FLAG-SPR to a final concentration

of 10 nM and 3 nM, respectively, in assay buffer (25 mM HEPES, pH 7.5, 150 mM NaCl, 0.01% Tween-20)

containing 10 nM SEP into a Corning 384-well white, low volume plate with a Thermo Multidrop Combi.

Inhibitors were dissolved in 100% DMSO to a top concentration of 5 mM and then serially diluted (1:2

stepwise) with 100% DMSO to generate a 22-point curve in a standard 384-well polypropylene plate. Assay

buffer supplemented with 10 µM NADPH was added to the inhibitor titration plate and the reaction was initiated

by transferring from the inhibitor titration plate to the assay plate using a Thermo Vprep liquid dispenser. The

final top concentration of inhibitor was 50 µM in the assay. The reaction was incubated for 40 min at room

temperature and stopped by the addition of sulfasalazine (to a final concentration of 10 µM). The detection

buffer NADP/NADPHGlo^{TM} was prepared and added to the stopped reaction as recommended by the

manufacturer (omitting the use of NADP cycling enzyme). After 45 min of incubation the plate was read on an

Envision 2104 Multimode Plate Reader (PerkinElmer) using the ultra-sensitive luminescence detection method.

Statistical Analyses

Since the von Frey filament set was calibrated on a logarithmic scale by the vendor (Stoelting), our selection of

9 filaments for the up-down method was also based on nearly equal logarithmic intervals, and because it is our

experience that variability noticeably increases with threshold value (Dixon, 1980), data were analyzed

following logarithmic transformation prior to statistical analysis. Actual gram values were plotted on a gram

scale Y-axis of the figures for convenience. Behavioral data are expressed as S.E.M. Results were analyzed

using one-way analysis of variance (ANOVA) with Dunnett's multiple comparisons post hoc test for significance

relative to vehicle. Statistical calculations and graphs were made using GraphPad Prism 7.01 (GraphPad

Software Inc., San Diego, CA, USA).

Results

Chemical Synthesis and Biochemical Inhibition of SPR Inhibitors

Literature evaluation of chemical matter revealed several molecules that have demonstrated biochemical inhibition of SPR as well as reduction in BH4 in vivo. Synthesis of these molecules was initiated; concurrently we developed a biochemical assay to assess in vitro potency of inhibition. The SPR NADPH-Glo assay IC_{50} determinations were consistent with reported values in Table 1 (Zhao et al., 2009; Latremoliere et al., 2015; Tebbe et al., 2017). Q-1195 was determined to be the most potent inhibitor of those tested. Thus, Q-1195 was moved forward into in vivo characterization to determine its suitability as a tool molecule to probe for behavioral and biochemical changes associated with SPR inhibition in vivo.

Bioanalytical Method

Accurate and reliable bioanalytical methods were required to monitor the pterin biomarkers associated with SPR inhibition. A coordinated series of method development steps were undertaken in a fit-for-purpose matter during bioanalytical method development. Several bioanalytical methods provided the basis for internal development efforts(Fukushima and Nixon, 1980b; Schmidt et al., 2006). Details of these investigations may be found in the Methods section. Briefly, stock solutions were prepared in 1:1 DMSO:Methanol, which resulted in a near 10-fold increase in MS response compared to aqueous and DMSO-alone solutions. A shallow LC gradient with methanol and water (containing 0.002% formic acid) was selected with separations performed on a Phenomenex Polar RP column. Stabilization of BH4 to BIO was achieved by oxidation of matrix (plasma or DRG) using I/KI in HCl solutions. Biological samples (plasma and DRG) were split and processed by two routes: 1, protein precipitation with Q-1195 detection in positive ion mode followed by immediate reanalysis of the samples for BIO and SEP in negative ion mode; 2, oxidation (I/KI in HCl) followed by SPE trapping for detection of BH4 measured as BIO (Figure 2).

Protein Binding Assessment

Fractional binding to plasma proteins and neural tissues was assessed by ultracentrifugation in effort to determine the unbound fraction (f_u) in separate tissues. Brain homogenates were used as a surrogate for

DRG (Liu et al., 2018). Attempts to determine $f_{u,DRG}$ were made, but these efforts proved challenging because the DRG homogenate would seize, making it unusable to liquid transfers. Fractional binding studies produced $f_{u,plasma} = 0.20$ and $f_{u,brain} = 0.32$.

PK Results

Q-1195 was administered to male Sprague-Dawley rats by i.v. and p.o. routes of administration and results are summarized in Table 2. Following i.v. administration (1.0 mg/kg), Q-1195 underwent first-order elimination, displayed low clearance (0.063 l/h/kg) and a long half-life (4.5 h). A low V_{ss} (0.4 l/kg) indicated that Q-1195 was primarily restricted to plasma water. P.o. administration (5 mg/kg) demonstrated good bioavailability (86.7%) with a C_{max} of 26.3 µM at 2 h post-dose. Based on these initial findings, Q-1195 was deemed suitable for subsequent p.o. dose-escalation studies. P.o. dose escalation at 15 mg/kg and 45 mg/kg indicated less than dose-proportional increases in AUC (Table 2). Additionally, repeat dosing of Q-1195 at 15 mg/kg for 3 days demonstrated minimal dose accumulation (Day 1 AUC_{inf} = 434 µM*h; Day 2 AUC_{inf} = 509 µM*h). A PK model was developed using Phoenix WinNonlin/NLME and adequately described the PK of Q-1195 (Figure 3); predicted concentrations correlated well with measured values ($R^2 = 0.91$). The plasma PK was 80% of dose-proportional between 5 and 15 mg/kg, and 46% of dose-proportional between 5 and 45 mg/kg, suggesting decreased bioavailability. The model estimations of bioavailability were consistent with this trend, fitting to 100% (CI: 80 to 120%) at 5 and 15 mg/kg and 58% (CI: 53 to 63%) at 45 mg/kg. PK parameter values and CI estimated with the model are shown in (Table 3).

PK/PD Results

Concomitant with the assessment of plasma concentrations of Q-1195, SEP was measured in plasma for each dose group (i.v. and p.o.). The appearance of SEP in plasma increased in response to increased p.o. exposure of Q-1195, indicating Q-1195 was engaged with its target (SPR) and that SPR inhibition was measurable in the plasma compartment (Figure 3). An indirect PK/PD model adequately described the relationship between plasma PK of Q-1195 and the plasma SEP levels (Figure 3). Predicted SEP levels correlated with measured values ($R^2 = 0.86$). The PK/PD derived in vivo SPR IC_{50} for inhibition of the conversion of SEP to BH4 by SPR

was 2.2 μM (Table 4), with the corresponding unbound in vivo SPR IC_{50} = 0.44 μM. The PD response was 80%

dose-proportional between 5 and 15 mg/kg and 74% dose-proportional between 5 and 45 mg/kg,

demonstrating that increased Q-1195 exposure led to an increase in SEP concentration. We then used the

indirect PK/PD model to project a dose that would cover the in vivo SPR IC_{90} at C_{min} for use in subsequent pain

studies. Results from the model projection indicated that a Q-1195 dose of 60 mg/kg dose yields plasma

concentrations at C_{min} exceeding 2.2 μM.

To determine the extent of SPR inhibition at the presumed site of action (DRG), SEP was measured in excised

DRG from intact rats. After p.o. dosing at 15 mg/kg, SEP levels in DRG increased from undetectable

(< 15 ng/g) in sham-dosed animals to 26.0 ng/g on Day 1 and 50.9 ng/g on Day 3. The corresponding plasma

concentrations of SEP were 20.8 and 19.1 ng/ml on Day 1 and Day 3, respectively. Q-1195 was measured in

the same DRG samples and found to be 9.1 nmol/g (9.1 μM) on Day 1 and 11.8 nmol/g (11.8 μM) on Day 3.

The corresponding plasma concentrations of Q-1195 were 29.6 and 30.7 μM on Day 1 and Day 3,

respectively.

Q-1195 Did Not Affect Open-field Activity

Potential analgesic effects of a new chemical entity can be confounded by behavioral changes that produce

sedative or motor side effects and may lead to a false positive response. Therefore, prior to testing in a pain

behavioral model, we evaluated Q-1195 in an open-field assessment to observe general behavior changes

after exposure to test article. Following 15 and 60 mg/kg p.o. administration of Q-1195, the mean plasma

concentrations at 3.5 h post-dose were 79.8 and 193 μM, respectively, while the SEP plasma concentration

was 41.1 and 59.8 ng/ml, respectively. The $C_{u,plasma}$ was 38.6 μM at the 60 mg/kg dose indicating that an

8.6-fold coverage of the unbound in vivo SPR IC_{90} was achieved near C_{max}. The 60 mg/kg projection from the

PK/PD model matched reasonably well to the data with both the Q-1195 and SEP falling within 2-fold of the

prediction (Figure 3). The measured Q-1195 plasma concentrations were 1.5-fold higher than projected

(130 μM), and the measured plasma SEP concentrations were 1.6-fold higher than projected (37.9 μM). At 3 h

post-dose, basic movement counts (5532 ± 165.7) were not significantly different relative to the vehicle-treated

group (5406 ± 386.2), and total rearing counts (184.4 ± 14.8) were not significantly different relative to the

vehicle-treated group (173.3 ± 15.1) (Figure 4A & 4B). Similarly, at the lower dosing group (15 mg/kg) no significant effect on basic movements or total rearing counts were observed. Results from the open-field assessment indicate that any behavioral change in the SNL assessment would likely be attributable to a pharmacological effect rather than an overt behavioral change.

Q-1195 Did Not Reverse SNL-induced Tactile Allodynia

Following no observable effect in the open-field assessment, Q-1195 was assessed for its ability to reverse tactile allodynia in the SNL rat pain model. Q-1195 was administered at 60 mg/kg p.o. for 3 consecutive days to SNL rats (n = 10); testing was assessed on Day 1 and reassessed on Day 3 to evaluate the pharmacological response from acute and repeat administration, respectively. The typical baseline, pre-surgery threshold for tactile response was 13.5 g. Two weeks after SNL surgery, sham-treated rats exhibited a tactile threshold of 2.53 ± 1.45 g (3 h post-single-dosing of vehicle) and 2.30 ± 1.71 g (3 h post-multi-dosing of vehicle on Day 3) indicating SNL surgery produced the expected endpoint of reduced pain threshold. Gabapentin (100 mg/kg p.o.) was administered as a positive control to separate cohorts of SNL rats on Day 1 or Day 3 of the experiment. Previous open-field assessment of gabapentin at this dose level was determined to have no impact on basic movements or rearing counts (negative in the open-field assessment). Gabapentin significantly reversed SNL-induced tactile allodynia with an increase in the tactile threshold to 8.94 ± 3.95 g (Day 1) and 10.12 ± 4.45 g (Day 3). Q-1195 at 60 mg/kg p.o. did not increase the tactile threshold relative to vehicle on either Day 1 or Day 3 of this multi-dose study (p > 0.05 by Dunnett's multiple comparisons test) with observed mean tactile thresholds of 2.61 ± 1.45 g and 2.94 ± 1.71 g on Day 1 and Day 3, respectively (Figure 4C).

Biochemical Assessment of SPR Inhibition in the SNL Rat

In addition to the von Frey behavioral response assessment of tactile threshold, biochemical endpoints of SPR inhibition (BH4 and SEP) were also evaluated. Plasma samples were collected after behavioral assessment (3.5 h post-dose) on Day 1 and Day 3 of the study and DRG were collected only at the termination of the study on Day 3. Vehicle-dosed animals were run as the negative control. Analysis of plasma samples (3.5 h post-

dose) from Day 1 and Day 3 demonstrated Q-1195 concentrations of 241 µM and 231 µM, respectively (Figure 4D). These plasma levels were consistent with (and slightly higher than) the measured plasma concentrations from the 60 mg/kg p.o. dose in the open-field activity assessment. The unbound in vivo IC_{90} coverage was determined to be 11-fold on both Day 1 and Day 3. Correspondingly, an increase in plasma SEP levels was observed in Q-1195-treated rats relative to the vehicle-dosed controls. SEP plasma concentrations increased from undetectable (LLOQ 1 ng/ml) in vehicle-treated rats to mean plasma levels of 46.1 ng/ml and 55.6 ng/ml on Day 1 and Day 3, respectively, following administration of Q-1195 (Figure 4E).

The anticipated site of pharmacological effect for Q-1195 is the SPR expressed in the DRG. The SNL procedure was performed on the left-side of the rat spine and was designated as the ipsilateral side, and the non-surgical (right-side) was labeled as the contralateral. Because SNL surgery was only applied to the ipsilateral side, the contralateral side served as an internal control to monitor changes in BH4. Quantitation of BH4 in the ipsilateral DRG of vehicle-dosed animals demonstrated a 6.7-fold increase relative to the contralateral DRG (from 18.5 to 124.7 ng/g) (Figure 4H), which indicated SNL surgery led to elevated BH4 levels as previously reported (Latremoliere et al., 2015). This is also in agreement with the decrease in tactile threshold observed during von Frey testing (described above). Analysis of the ipsilateral DRG from Q-1195-dosed animals demonstrated a 59% reduction in BH4 levels relative to sham-dosed controls (from 124.7 to 51.5 ng/g). Despite this decrease in BH4 in Q-1195-exposed rats, there was no significant increase in tactile threshold observed during von Frey testing. In good agreement with the decrease in BH4 in the ipsilateral DRG following exposure to Q-1195, levels of SEP were significantly increased over sham-dosed DRGs from BQL to 156.8 ng/g in ipsilateral DRG and 57.6 ng/g in contralateral DRG (Figure 4G). Analysis of DRG on Day 3 revealed the presence of Q-1195 at levels of 26.8 µM (Figure 4F). The $C_{u,DRG}$ for Q-1195 was 8.6 µM 3.5 h post-dose, which was in excess of the unbound in vivo SPR IC_{90} by 2-fold.

Discussion

To support the early pipeline and evaluate novel non-opioid targets for analgesia, we developed a fit-for-purpose analysis suite to quantify both test article and relevant target-specific biomarkers in a pharmacological model of pain sensitivity. The requirement to generate data for multiple analytes from

low-volume rodent samples presented several analytical challenges. The methods reported here accommodated the analysis of BIO and SEP in plasma using the same negative ion acquisition method. Q-1195, along with other test articles, in plasma was successfully analyzed by immediate re-injection of the sample plates employing a positive ion acquisition method. BIO, SEP and Q-1195 were quantitated in DRG matrix using the same methods used in the analysis of plasma samples. The oxidation reaction implemented to convert BH4 to BIO required a second sample preparation event in both plasma and DRG samples for quantitation of BH4. The methods reported here allowed for the rapid turnaround of bioanalytical results for BH4, BIO, SEP and Q-1195 in both plasma and DRG samples. The turnaround time for the complete analysis of a behavioral (SNL) study including sample preparation, data analysis and report generation was approximately 4 days.

The DRG matrix presented unique sample handling challenges. Homogenates were prepared for both matrix spiking of analytical standard curves as well as for the analysis of in vivo samples. Homogenates of DRG were typically prepared as 2:1 mixtures of PBS:tissue. Gradually, these mixtures would seize and become unworkable to any subsequent liquid transfers, and it became impossible to determine fractional binding in DRG by ultracentrifugation because a total recovery sample could not be reproducibly transferred due to these severe matrix effects. Homogenates diluted 10:1 in PBS:tissue produced similar results. However, when total recovery was desired, precipitation and extraction with organic solvent (acetonitrile) was successful as evidenced by the linearity of spiked standard curves used for bioanalysis. Liu et al. recently reported strong correlation in fractional binding among neural tissues (brain, spinal cord, sciatic nerve and DRG) by using rapid equilibrium dialysis (Liu et al., 2018). Dialysis was not attempted in our analysis, but it's possible that congealing events observed in our studies may be overcome using dialysis, provided the solidified DRG matrix permitted small molecule equilibrium to be achieved between dialysis solution reservoirs.

Application of these bioanalytical methods to preclinical studies enabled reliable determinations of test article and pterin metabolites in both plasma and DRG. Collectively, this provided a quantitative basis to derive PK/PD relationships and assess pharmacological inhibition of SPR in a rat model of neuropathic pain. Using the PK analysis and PK/PD projections, the unbound plasma concentrations from a 60 mg/kg p.o. dose in the

SNL experiment was designed to exceed the in vivo SPR IC_{90} at C_{min} over the dose interval. Plasma quantitation of Q-1195 in the SNL experiment demonstrated the unbound plasma concentrations exceeded the unbound in vivo SPR IC_{90} by 11-fold at 3.5 h post-dose (the approximate C_{max}). The PK model projection at 3.5 h post-dose projected 6.8-fold coverage of the in vivo SPR IC_{90}. Thus, we inferred that unbound plasma concentrations exceeded the in vivo unbound IC_{90} at C_{min} as well and was consistent with the projections.

The opportunity to assess target engagement (SPR inhibition) through SEP appearance in a typical p.o. PK experiment was very attractive. The PK/PD model produced a reliable prediction of SPR inhibition and likely would have been a useful tool in a drug discovery campaign, provided a relationship between PD and efficacy was established. This approach would have minimized the reliance on SNL studies, which are time and resource intensive. Prioritizing compounds based off both PK and PD early in the discovery flow scheme likely would have provided an efficient use of resources, where by the SNL studies would have been reserved for true lead candidates, and greater confidence in the outcomes would be expected.

There was a large difference in potency observed between the calculated in vitro rat SPR IC_{50} (0.004 µM) and the in vivo SPR IC_{50} (2.2 µM and unbound in vivo SPR IC_{50} = 0.44 µM) of approximately 110-fold. Prior studies demonstrated a strong right-shift in potency from biochemical to cell for human SPR with SPRi3 of approximately 70-fold (not adjusted for fractional binding in the cell-based assay) (Latremoliere et al., 2015). Large shifts in potency from biochemical to cell-based assays are common; further, shifts from cell-based potency to in vivo potency are frequently right-shifted. The biochemical, recombinant protein-based assay is largely a measure of potency and may not fully account for mode of action and intracellular compartment effects that would be increasingly prevalent from cell culture to in vivo. In the absence of a reliable cell-based potency assessment, we used the calculated in vivo assessment of SPR inhibition (measured by the increase in SEP in plasma) to benchmark the target coverages for the determination of efficacy in the SNL investigation.

Despite biochemical evidence for inhibition of SPR in both plasma and DRG, there was no observable increase in tactile paw withdrawal to SNL rats. The reason for this lack of behavioral change is unclear, but several explanations are possible. A possible disconnect between the unbound plasma coverage and behavior effect may result from unanticipated differences in unbound concentrations of test article in the DRG. SEP, BH4 and

Q-1195 were all quantified in DRG; increased levels of SEP were observed as well as a decrease in BH4, which suggested that SPR inhibition was achieved in DRG. Total concentrations of Q-1195 were measured in DRG, but the unbound fraction estimates were determined from brain matrix studies ($f_{u,brain}$). Even though there appears to be a strong relationship between fractional binding in brain relative to DRG (Liu et al., 2018), it's possible that some chemotypes will deviate from this relationship. If the actual $f_{u,DRG}$ was 10-fold lower than $f_{u,plasma}$ then it's conceivable that in DRG only the in vivo SPR IC_{50} was exceeded at C_{min}. However, fractional binding was also evaluated in spinal cord and nerve homogenates with Q-1195 and these values were within 2-fold of the $f_{u,brain}$ value (data not shown), which is consistent with prior reports (Liu et al., 2018). Penetration into the tissue could also impact the local concentration; however, in vitro permeability assessment of Q-1195 in parental MDCK cell monolayers indicated favorable passive permeability (P_{app} = 15 µcm/s, data not shown), which should not be limiting for tissue distribution. BH4 levels in healthy DRG were generally in the 20 to 30 ng/g range. SNL surgery caused an increase in BH4 that was greater than 100 ng/g. There was often a tight S.D. around the measured levels but a large range of values within a given experiment. This heterogeneity in response may also have impacted our ability to effectively reduce BH4. A 60% reduction in BH4 was observed following exposure to Q-1195 and it's possible that a larger magnitude of BH4 reduction is required to return animals to their tactile threshold baseline. It's worth noting that even for the positive control, gabapentin, there was a large variation in tactile threshold response (ranging from 2.32 to 15.0 g). A large sample number (n = 10 rats) for all SNL groups was used to gain a better estimate of the sample mean. Though not evaluated in this study, the selection of rodent strains and vendors can impact physiological and behavioral endpoints in preclinical studies. Additionally, several neuropathic pain models are used in preclinical research; it's possible that varied results could be observed with SNL, spared nerve injury or chronic constriction injury models. Behavioral models often exhibit large variability in response (pain models included) that present additional obstacles in the drug discovery pipeline.

Acknowledgements

Public Information

Authorship contributions

Participated in research design: Meyer, Sparling, McCarty, Zhang, Soto, Schneider, Tan, Kornecook, Andrews, Knutson

Conducted experiments: Meyer, Sparling, McCarty, Zhang, Soto, Schneider, Chen, Roberts, Tan

Contributed new reagents or analytical tools: Meyer, Sparling, McCarty, Schneider, Chen

Performed data analysis: Meyer, Sparling, McCarty, Zhang, Schneider, Roberts, Tan, Kornecook, Andrews, Knutson

Wrote or contributed to the writing of the manuscript: Meyer, Sparling, McCarty, Zhang, Soto, Schneider, Chen, Roberts, Tan, Kornecook, Andrews, Knutson

References

Administration USFaD (2013) Guidance for Industry: Bioanalytical Method Validation.

Arning E and Bottiglieri T (2016) LC-MS/MS Analysis of Cerebrospinal Fluid Metabolites in the Pterin Biosynthetic

Pathway. *JIMD reports* **29:**1-9.

Chaplan SR, Bach FW, Pogrel JW, Chung JM, and Yaksh TL (1994) Quantitative assessment of tactile allodynia in the rat

paw. *Journal of neuroscience methods* **53:**55-63.

Cowan K, Gao X, Parab V, Nguy T, Wu L, Arron JR, Townsend M, Wallin J, Cheu M, Morimoto A, and Wakshull E (2016)

Fit-for-purpose biomarker immunoassay qualification and validation: three case studies. *Bioanalysis*.

Cummings J, Ward TH, Greystoke A, Ranson M, and Dive C (2008) Biomarker method validation in anticancer drug

development. *British journal of pharmacology* **153:**646-656.

Dixon WJ (1980) Efficient analysis of experimental observations. *Annual review of pharmacology and toxicology* **20:**441-

462.

Fismen L, Eide T, Djurhuus R, and Svardal AM (2012) Simultaneous quantification of tetrahydrobiopterin,

dihydrobiopterin, and biopterin by liquid chromatography coupled electrospray tandem mass spectrometry.

Anal Biochem **430:**163-170.

Fukushima T and Nixon JC (1980a) Analysis of reduced forms of biopterin in biological tissues and fluids. *Anal Biochem*

102:176-188.

Fukushima T and Nixon JC (1980b) Chromatographic analysis of pteridines. *Methods Enzymol* **66:**429-436.

Hatakeyama K, Inoue Y, Harada T, and Kagamiyama H (1991) Cloning and sequencing of cDNA encoding rat GTP

cyclohydrolase I. The first enzyme of the tetrahydrobiopterin biosynthetic pathway. *The Journal of biological*

chemistry **266:**765-769.

Kalvass JC, Maurer TS, and Pollack GM (2007) Use of plasma and brain unbound fractions to assess the extent of brain

distribution of 34 drugs: comparison of unbound concentration ratios to in vivo p-glycoprotein efflux ratios.

Drug metabolism and disposition: the biological fate of chemicals **35:**660-666.

Kim HR, Kim TH, Hong SH, and Kim HG (2012) Direct detection of tetrahydrobiopterin (BH4) and dopamine in rat brain using liquid chromatography coupled electrospray tandem mass spectrometry. *Biochemical and biophysical research communications* **419:**632-637.

Kim SH and Chung JM (1992) An experimental model for peripheral neuropathy produced by segmental spinal nerve ligation in the rat. *Pain* **50:**355-363.

Latremoliere A and Costigan M (2011) GCH1, BH4 and pain. *Curr Pharm Biotechnol* **12:**1728-1741.

Latremoliere A, Latini A, Andrews N, Cronin SJ, Fujita M, Gorska K, Hovius R, Romero C, Chuaiphichai S, Painter M, Miracca G, Babaniyi O, Remor AP, Duong K, Riva P, Barrett LB, Ferreiros N, Naylor A, Penninger JM, Tegeder I, Zhong J, Blagg J, Channon KM, Johnsson K, Costigan M, and Woolf CJ (2015) Reduction of Neuropathic and Inflammatory Pain through Inhibition of the Tetrahydrobiopterin Pathway. *Neuron* **86:**1393-1406.

Leonard M, Dunn J, and Smith G (2014) A clinical biomarker assay for the quantification of d3-creatinine and creatinine using LC-MS/MS. *Bioanalysis* **6:**745-759.

Liu H, Chen Y, Huang L, Sun X, Fu T, Wu S, Zhu X, Zhen W, Liu J, Lu G, Cai W, Yang T, Zhang W, Yu X, Wan Z, Wang J, Summerfield SG, Dong K, and Terstappen GC (2018) Drug Distribution into Peripheral Nerve. *J Pharmacol Exp Ther* **365:**336-345.

Mager DE, Wyska E, and Jusko WJ (2003) Diversity of mechanism-based pharmacodynamic models. *Drug metabolism and disposition: the biological fate of chemicals* **31:**510-518.

National Research Council (U.S.). Committee for the Update of the Guide for the Care and Use of Laboratory Animals., Institute for Laboratory Animal Research (U.S.), and National Academies Press (U.S.) (2011) Guide for the care and use of laboratory animals, pp xxv, 220 p., National Academies Press,, Washington, D.C.

Rudd RA, Seth P, David F, and Scholl L (2016) Increases in Drug and Opioid-Involved Overdose Deaths - United States, 2010-2015. *MMWR Morbidity and mortality weekly report* **65:**1445-1452.

Schmidt H, Tegeder I, and Geisslinger G (2006) Determination of neopterin and biopterin by liquid chromatography coupled to tandem mass spectrometry (LC-MS/MS) in rat and human plasma, cell extracts and tissue homogenates.

Stea B, Halpern RM, Halpern BC, and Smith RA (1980) Quantitative determination of pterins in biological fluids by high-performance liquid chromatography. *J Chromatogr* **188:**363-375.

Tebbe MJ, Atton HV, Avery C, Bromidge SM, Kerry M, Kotey AK, Monck NJ, Meniconi M, Ridgill MP, Tye H, Saiah E, Johnsson KP, Gorska KI, Peng H, and McCall JM (2017) Preparation of heteroaryl derivatives as sepiapterin reductase inhibitors, pp 356pp., Quartet Medicine, Inc., USA; Ecole Polytechnique Federale de Lausanne EPFL .

Tegeder I, Costigan M, Griffin RS, Abele A, Belfer I, Schmidt H, Ehnert C, Nejim J, Marian C, Scholz J, Wu T, Allchorne A, Diatchenko L, Binshtok AM, Goldman D, Adolph J, Sama S, Atlas SJ, Carlezon WA, Parsegian A, Lotsch J, Fillingim RB, Maixner W, Geisslinger G, Max MB, and Woolf CJ (2006) GTP cyclohydrolase and tetrahydrobiopterin regulate pain sensitivity and persistence. *Nat Med* **12:**1269-1277.

Volkow ND, Frieden TR, Hyde PS, and Cha SS (2014) Medication-assisted therapies--tackling the opioid-overdose epidemic. *The New England journal of medicine* **370:**2063-2066.

Yang S, Jan YH, Mishin V, Richardson JR, Hossain MM, Heindel ND, Heck DE, Laskin DL, and Laskin JD (2015) Sulfa drugs inhibit sepiapterin reduction and chemical redox cycling by sepiapterin reductase. *J Pharmacol Exp Ther* **352:**529-540.

Zhao Y, Cao J, Chen YS, Zhu Y, Patrick C, Chien B, Cheng A, and Foehr ED (2009) Detection of tetrahydrobiopterin by LC-MS/MS in plasma from multiple species. *Bioanalysis* **1:**895-903.

Figures Legends

Figure 1. BH4 de novo synthesis and salvage pathways. Sepiapterin reductase (SPR) catalyzes the conversion of sepiapterin (SEP) to tetrahydrobiopterin (BH4). Exogenous oxidation (I/KI in HCl) or non-enzymatic oxidation ([O]) facilitates the conversion of BH4 to biopterin (BIO). GCH1, GTP cyclohydrolase 1; 6PTS, 6-pyruvoyl-tetrahydrobiopterin synthase; AR, aldose reductase; CR, carbonyl reductase; DHFR, dihydrofolate reductase.

Figure 2. Biomarker bioanalytical work flow. Starting from either plasma or DRG tissues, samples were split into 2 fractions. The first fraction was subject to protein precipitation with acetonitrile, followed by evaporation to dryness under N_2, then reconstitution in mobile phase for LC-MS/MS analysis in positive ion mode to quantify inhibitor, and followed by immediate reanalysis of the samples in negative ion mode for analysis of BIO and SEP. The second fraction was oxidized (I/KI in HCl) to convert BH4 to BIO, followed by SPE trapping, elution, evaporation to dryness under N_2, and reconstitution in mobile phase for LC-MS/MS analysis in negative ion mode.

Figure 3. PK/PD model fits and projections compared to observed data. (A) Schematic of the inhibition of dissipation indirect effect model. (B) Plasma concentrations of Q-1195 after oral doses of 5 (●), 15 (x), and 45 mg/kg (Δ) were fit to a one-compartmental extravascular model (best-fit lines shown). (C) SEP levels over time after dosing Q-1195. (C & D) Plasma concentrations of Q-1195 and SEP were then fit to the indirect PK/PD model [best-fit lines (solid lines) and 95% CI (dotted lines) are shown for a 60 mg/kg p.o. dose]. The model was used to predict plasma concentrations of Q-1195 (D) and SEP (E) after a 60 mg/kg oral dose. Experimental data from the open-filed activity assessment (●) and SNL (○) experiments are shown. The in vivo SPR IC_{90} (22 μM) is shown in panel (D) (gray horizontal line).

Figure 4. Behavioral and biochemical assessment in SNL rats following PO administration of Q-1195. (A & B) Open-field activity assessment of basic movements and total rearing counts was assessed in male Sprague-Dawley rats following p.o. administration of Q-1195 at 15 mg/kg and 60 mg/kg (n = 8 per group). Neither basic movements nor total rearing counts were statistically different from vehicle-treated controls at

either dose level of Q-1195. (C) Reversal of SNL-induced tactile allodynia was assessed 3 h post-dose on Day 1 and Day 3 following QD p.o. administration of 60 mg/kg Q-1195. Vehicle-treated SNL rats exhibited a tactile threshold of 2.53 ± 1.45 g and 2.30 ± 1.71 g on Day 1 and Day 3, respectively. SNL rats treated with 60 mg/kg Q-1195 displayed a tactile threshold of 2.61 ± 1.45 g and 2.94 ± 1.71 g on Day 1 and Day 3, respectively, which was indistinguishable from vehicle-treated controls. SNL rats treated with 100 mg/kg gabapentin displayed a tactile threshold of 8.94 ± 3.95 g and 10.12 ± 4.45 g on Day 1 and Day 3, respectively, which was statistically different from vehicle-treated controls. (D & E) LC-MS/MS analysis of plasma samples from Q-1195-treated SNL rats demonstrated exposure to Q-1195 (241 µM and 231 µM on Day 1 and Day 3, respectively) and elevations in SEP (46.1 ng/ml and 55.6 ng/ml on Day 1 and Day 3, respectively) relative to vehicle-treated controls. (F & G) Q-1195 was quantified in DRG on Day 3 and determined to be 26.8 µM; SEP levels in the ipsilateral and contralateral DRG of SNL rats were 156.8 ng/ml and 57.6 ng/ml, respectively, upon exposure to Q-1195 at 60 mg/kg p.o. for 3 consecutive days. (H) LC-MS/MS analysis of DRG samples from Q-1195-treated SNL rats demonstrated a 60% reduction in BH4 from 124.7 to 51.5 ng/ml relative to vehicle control in the ipsilateral DRG ($p = 0.008$). In the vehicle-treated group, BH4 was elevated in the ipsilateral DRG but not the contralateral DRG ($p<0.0001$). Ispi; ipsilateral. Contra; contralateral.

Table 1. Biochemical assessment of SPR inhibition with recombinant rat and human SPR protein. A

minimum of 3 replicates were used to determine the mean and S.D. for each inhibitor.

Inhibitor	Rat SPR IC$_{50}$ (µM)	Human SPR IC$_{50}$ (µM)	Human SPR (µM) Reference
Sulfasalazine	0.100 +/- 0.046	0.016 +/- 0.004	0.031 (Yang et al., 2015)
SPRi3	0.014 +/- 0.007	0.062 +/- 0.021	0.074 (Latremoliere et al., 2015)
Q-1195	0.004 +/- 0.001	0.008 +/- 0.001	0.002 (Tebbe et al., 2017)

Table 2. PK parameters for Q-1195 following i.v. and p.o. dosing in Sprague-Dawley rats.

Route	Dose	AUC_{inf}[1]	CL[2]	V_{ss}[3]	$t_{1/2}$[4]	%F[5]
	(mg/kg)	(µM*h)	(l/h/kg)	(l/kg)	(h)	
i.v.[6]	1.0	42.3	0.063	0.4	4.5	
p.o.[6]	5.0	183			5.5	87
p.o.[6]	15[6]	434			9.1	
p.o.[6]	15[7]	509			9.0	
p.o.[6]	45	850			7.8	
		AUC_t	AUC_t/dose	AUC_t/AUC_t low dose	% of linear	%F
p.o.[9]	5	194	39	1.0	100	100
p.o.[9]	15	464	31	2.4	80	100
p.o.[9]	45	797	18	4.1	46	58

[1]AUC_{inf}, area under the curve to infinity

[2]CL; clearance

[3]V_{ss}; volume of distribution at steady state

[4]$t_{1/2}$; half-life

[5]%F, bioavailability

[6]Pharmacokinetic parameters determined by non-compartment analysis

[7]Day 1

[8]Day 3

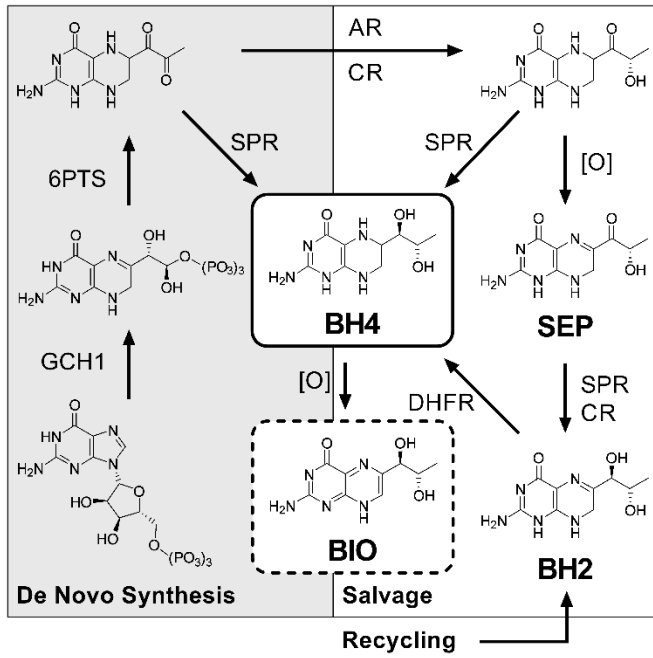[9]AUC_t, area under the curve to last time point

[10]Pharmacokinetic parameters determined from a 1-compartment model

Table 3. Best-fit PK/PD model parameters.

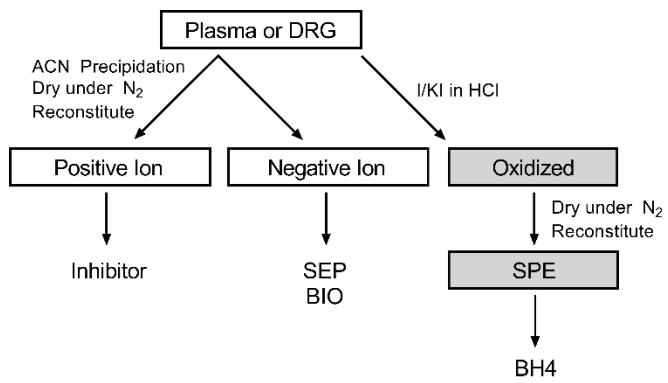| Parameter	Description	%CV	Mean	95% CI
k_a	Adsorption rate	20	2.5 1/h	1.5-3.6 1/h
V	Volume of distribution	8.9	0.92 l/kg	0.76-1.1 l/kg
CL	Clearance	2.9	0.075 l/h/kg	0.071-0.079 l/h/kg
k_{in}	SEP synthesis rate	9.6	18 µg/l/h	14-21 µg/l/h
k_{out}	Baseline rate of SEP conversion to BH4	26	14 1/h	7.0-22 1/h
IC_{50}	Concentration at half-maximal inhibition	29	2.2 µM	0.89-3.5 µM

Figure 1.

Figure 2.

Public Information

Figure 3.

Public Information

Figure 4.